UC Irvine
UC Irvine Previously Published Works

Title

Stem Cell Transplantation Reverses Chemotherapy-Induced Cognitive Dysfunction

Permalink

https://escholarship.org/uc/item/8xh5q9r7

Journal

Cancer Research, 75(4)

ISSN

0008-5472

Authors

Acharya, Munjal M
Martirosian, Vahan
Chmielewski, Nicole N
et al.

Publication Date

2015-02-15

DOI

10.1158/0008-5472.can-14-2237

Peer reviewed

Stem Cell Transplantation Reverses Chemotherapy-Induced Cognitive Dysfunction

Munjal M. Acharya, Vahan Martirosian, Nicole N. Chmielewski, Nevine Hanna, Katherine K. Tran, Alicia C. Liao, Lori-Ann Christie, Vipan K. Parihar, and Charles L. Limoli

Abstract

The frequent use of chemotherapy to combat a range of malignancies can elicit severe cognitive dysfunction often referred to as "chemobrain," a condition that can persist long after the cessation of treatment in as many as 75% of survivors. Although cognitive health is a critical determinant of therapeutic outcome, chemobrain remains an unmet medical need that adversely affects quality of life in pediatric and adult cancer survivors. Using a rodent model of chemobrain, we showed that chronic cyclophosphamide treatment induced significant performance-based decrements on behavioral tasks designed to interrogate hippocampal and cortical function. Intrahippocampal transplantation of human neural stem cells resolved all cognitive impairments when animals were tested 1 month after the cessation of chemotherapy. In transplanted animals, grafted cells survived (8%) and differentiated along neuronal and astroglial lineages, where improved cognition was associated with reduced neuroinflammation and enhanced host dendritic arborization. Stem cell transplantation significantly reduced the number of activated microglia after cyclophosphamide treatment in the brain. Granule and pyramidal cell neurons within the dentate gyrus and CA1 subfields of the hippocampus exhibited significant reductions in dendritic complexity, spine density, and immature and mature spine types following chemotherapy, adverse effects that were eradicated by stem cell transplantation. Our findings provide the first evidence that cranial transplantation of stem cells can reverse the deleterious effects of chemobrain, through a trophic support mechanism involving the attenuation of neuroinflammation and the preservation host neuronal architecture. *Cancer Res; 75(4); 676–86. ©2015 AACR.*

Introduction

Advanced stage cancer treatments invariably involve some form of chemotherapy and/or radiotherapy that are useful in controlling both local and distal tumor growth. Efficacy of these treatments depends on the differential deposition of genotoxic damage between cancer cells and normal tissue, with the goal of minimizing injury to normal tissue while maximizing the death of cancer cells. Over the years, oncologists have dramatically improved long-term survival rates with over 12 million cancer survivors in the United States alone (1). Unfortunately, longer-term survival comes at a cost, as there are now numerous clinical (2, 3) and preclinical studies (4–6) that have established the debilitating side effects of cancer therapies on cognition. The situation is confounded further by the conspicuous absence of any satisfactory treatments for reducing the progressive neurocognitive sequelae associated with cancer therapies, and is a particularly pressing problem for pediatric cancer survivors (7, 8), where one in 640 young adults in the United States is estimated to be a pediatric cancer survivor (9). Thus, with the

exception of survival, cognitive function following cancer treatment may be the most critical criterion for evaluating therapeutic outcome and for determining long-term quality of life (10, 11).

Chemotherapy can lead to severe impairments in cognition that persist long after termination of treatment in as many as 75% of survivors (reviewed in ref. 12). The cognitive domains that are disrupted are diverse and include memory, processing speed, attention, and executive function (reviewed in refs. 11, 13). Although there is growing clinical literature describing this devastating syndrome, often referred to as "chemobrain" or "chemo fog," the precise mechanisms underlying chemotherapy-induced cognitive decline, as well as the contribution of patient-to-patient differences such as disease status, genetic background, and treatment strategy, remain unknown. While past work has clearly defined the sensitivity of neurogenic populations of neural progenitor cells to radiation (14) and chemotherapeutic agents (4, 15), it remains difficult to ascribe the spectrum of cognitive deficits to the loss of newly generated neurons in the hippocampus. Recent work analyzing the structure of newly born and mature hippocampal neurons has found irradiation (16, 17) to elicit marked reductions in dendritic complexity, spine density, and synaptic protein levels. Morphologic alterations were temporally coincident with impaired cognition (18), suggesting a cause and effect between altered neuronal anatomy and cognitive function. This idea is supported by a wealth of data that have linked perturbations in neuronal structure and synaptic integrity to the onset, progression and severity of a number of neurodegenerative diseases, including age-associated dementia (19–21).

To address some of the unresolved issues regarding the mechanistic basis of chemotherapy-induced cognitive dysfunction and to provide potential clinical recourse to those so afflicted, we explored the use of stem cell transplantation using a preclinical

Department of Radiation Oncology, University of California, Irvine, California.

Corresponding Author: Charles L. Limoli, Department of Radiation Oncology, University of California Irvine, Medical Sciences I, Room B-146B, Irvine, CA 92697-2695. Phone: 949-824-3053; Fax: 949-824-3566; E-mail: climoli@uci.edu
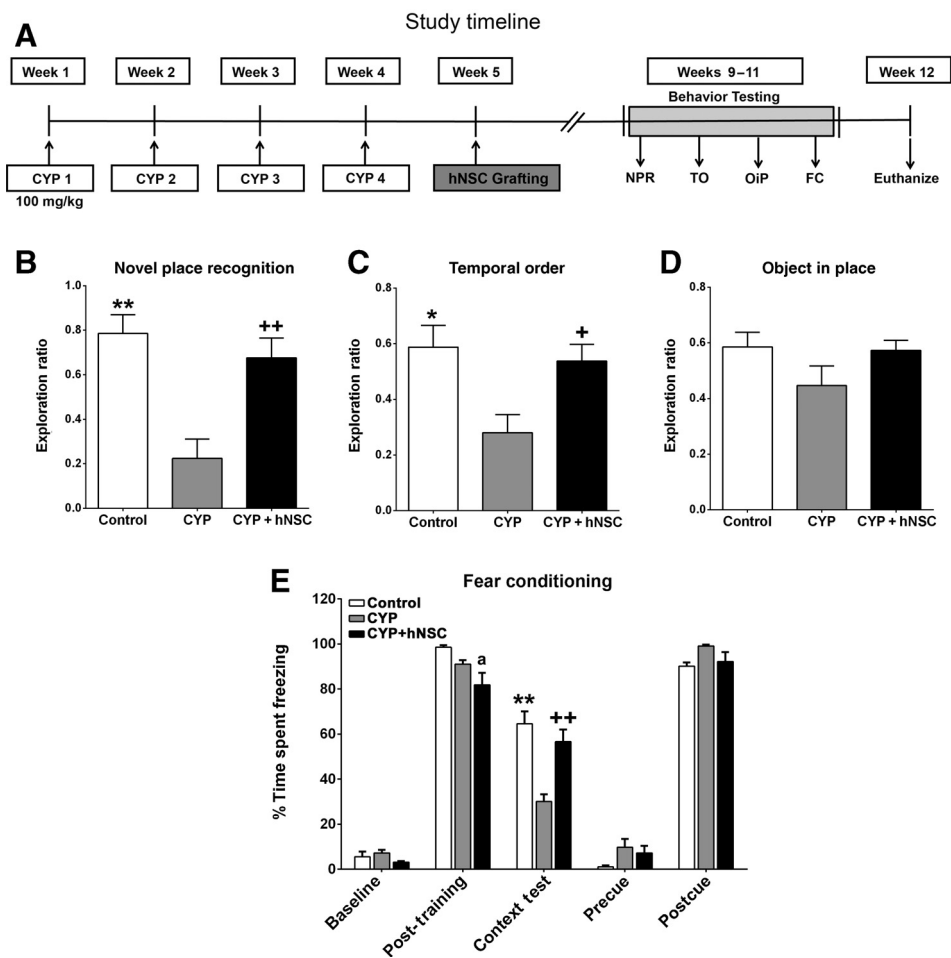
AACR

Figure 1.
Stem cell grafting improves behavioral performance after chronic chemotherapy. Engraftment of hNSCs improves behavioral performance 1 month after cessation of chronic CYP treatments and transplantation surgery. A, schematic of the experimental timeline showing four consecutive CYP treatments (100 mg/kg, once weekly) followed by hNSC grafting (week 5), behavioral testing (weeks 9–11) for the NPR, TO, OiP, and contextual and cued FC tasks. After completion of cognitive testing (week 12), animals were euthanized and brains were harvested for the immunohistochemistry and neuron morphology analysis. B, CYP treatment significantly impaired exploration on a NPR task compared with controls and grafted cohorts (CYP+hNSC) that were not statistically different. C, CYP treatment impaired preference of prior objects on a TO task compared with controls and grafted cohorts that were not statistically different. D, animals subjected to CYP treatment exhibit a trend of altered preference for objects at new locations on an OiP task, but were not found to be statistically different compared with other cohorts. E, one day after baseline and posttraining freezing levels were established, a context test was administered, where CYP-treated cohorts spent significantly decreased percentages of time freezing compared with the control and grafted cohorts (context test bars; E), which were not found to differ. After the initial training phase (48 hours), the context was changed, which resulted in a substantial reduction in freezing behavior (precue bars, E) that was restored following the tone sound (postcue test bars; E), indicating intact amygdala function in all groups. All data are presented as mean $\pm$ SEM ($N = 8$ animals each group). *, $P = 0.01$; **, $P = 0.001$; +, $P = 0.04$; ++, $P = 0.002$ compared with CYP group; a, $P = 0.01$ compared with the control group (ANOVA and Bonferroni multiple comparisons test).

model of chemobrain. This model has been successfully used to reverse the adverse effects of irradiation on cognition and has been adapted here to determine how cranial transplantation of human neural stem cells (hNSC) might ameliorate cognitive impairments caused by chronic administration of cyclophosphamide (CYP). Here, we report the beneficial neurocognitive effects of hNSC cranially grafted in our rodent model of chemobrain, effects caused in part, by the suppression of neuroinflammation and the preservation of host neuronal structure.

Materials and Methods

Detailed methods and procedures are provided in the Supplementary Data.

Animals and chemotherapy

Four-month-old athymic nude (ATN) rats (Cr:NIH-Foxn1[rnu], strain 316; Charles River) were divided into three groups ($n = 8$/ group): saline-treated controls receiving sham surgery (CON), cyclophosphamide-treated sham surgery (CYP), and CYP with hNSCs grafted 1 week following the final CYP injection (CYP + hNSC). Cyclophosphamide (Sigma-Aldrich) was dissolved in buffered saline and delivered (i.p.) in four doses (100 mg/kg) once weekly as shown in the study timeline (Fig. 1A).

Transplantation surgery

The use of human stem cells was approved by the Institutional Human Stem Cell Research Oversight Committee. The validation,

expansion, and characterization of hNSCs (ENStem-A; EMD Millipore) used for transplantation followed previously published procedures (22, 23). After CYP treatment, each rat received bilateral, intrahippocampal transplantation of 100,000 live hNSCs (passages 4–8) in 1 μL of cell suspension using a 33-gauge microsyringe at an injection rate of 0.25 μL/minute. Each hippocampi received 4 distinct injections (total 4.0×10^5 live cells per hemisphere) using precise stereotaxic coordinates, as described previously (24). Sham-surgery controls and drug-treated cohorts received sterile vehicle (hibernation buffer) at the same stereotaxic coordinates. Animals were anesthetized using isoflurane (5% induction, 2.5% maintenance; VetEquip).

Cognitive testing

To evaluate the outcome of hNSC transplantation on cognitive function, rats from each cohort (CON, CYP, and CYP+hNSC) were subjected to cognitive testing 1 month after transplantation surgery. Cognitive testing was conducted over 3 weeks and included 3 different open arena tasks followed by contextual and cued fear conditioning (FC). All trials were later hand scored by an independent observer blind to the experimental groups, where the average of those scores was used to compute all behavioral data. Open arena testing consisted of novel place recognition (NPR) followed by a temporal order (TO) then an object in place (OIP) task. For all arena tasks, a positive score was counted only when the nose of the rat was within 1 cm and pointed in the direction of the object. The time spent exploring novelty (place and/or object) was used as the main dependent measure for all arena testing. Data were used to derive an exploration ratio calculated as the time spent exploring the novel object divided by the total exploration time ($t_{novel}/t_{novel} + t_{familiar}$), as described previously (24). Additional details on animal behavior experiments are provided in the Supplementary Data.

Graft survival and differentiation, neuroinflammation, and morphometric analyses of neurons

Animals subjected to behavioral testing were segregated equally for morphometric or immunohistochemical analyses. Procedures for the assessment of graft survival, differentiation, neuroinflammation, ultrastructural analyses of Golgi–Cox impregnated neurons, including dendritic spines, are described in detail in the Supplementary Data.

Statistical analyses

Statistical analyses were carried out using PASW Statistics 18 (SPSS, IBM Corporation) and GraphPad Prism (v6). One-way ANOVA was used to assess significance between groups. When overall group effects were found to be statistically significant, a Bonferroni multiple comparisons test was used to compare the individual groups. For analysis of Sholl data (i.e., at specific distances from the soma), repeated measures two-way ANOVA were performed. All analyses considered a value of $P \leq 0.05$ to be statistically significant.

Results

Behavioral testing: novel place-recognition task

One month after transplantation, animals were habituated and tested on the NPR task (Fig. 1B). For the NPR task, total exploration of objects during the familiarization phase was not found to differ between the cohorts. Similarly, the total exploration time spent at either object during the test phase was not found to be statistically different. Group means and 95% confidence intervals (CI) for the exploration ratio were as follows: control (CON, mean = 0.785; 95% CI, 0.58–0.99); CYP (mean = 0.224; 95% CI, 0.017–0.43); CYP+hNSC (mean = 0.676; 95% CI, 0.47–0.88). A significant overall group effect was found ($F_{(2,21)} = 11.69$; $P = 0.0004$) for the exploration ratio to differ between the groups. After a 1-hour retention interval, CYP animals spent a significantly lower proportion of time exploring the novel place compared to CON ($P = 0.0005$) and CYP+hNSC ($P = 0.0043$) groups (Fig. 1B). On the other hand, after the 1-hour retention interval, CYP+hNSC animals did not differ from CON animals. Moreover, one-sample t tests comparing the exploration ratios of individual groups to chance (i.e., 0.5) revealed that CON ($P < 0.05$) and CYP+hNSC ($P < 0.05$) groups spent significantly more time exploring the novel place than expected by chance, while CYP animals explored the novel spatial location less than expected by chance ($P < 0.05$). Data indicate that hNSC transplantation improved exploration behavior after CYP treatment compared with CYP-treated animals not receiving stem cells.

Temporal order

After NPR testing, animals were habituated and subjected to a TO task (Fig. 1C). After familiarization with two sets of objects presented 4 hours apart (sample phases 1 and 2), animals were subjected to the test phase 1 hour after sample phase 2, using copies of the objects presented earlier (i.e., 1 or 5 hours before). Total exploration of the objects during the familiarization and test phases were reduced significantly after CYP treatment (i.e., CYP and CYP+hNSC cohorts) compared to controls. Animals with intact hippocampal function show preference for the original (5 hours prior) object.

Group means and 95% CIs for the exploration ratio were as follows: control (mean = 0.588; 95% CI, 0.40–0.77); CYP (mean = 0.280; 95% CI, 0.13–0.43); CYP+hNSC (mean = 0.538; 95% CI, 0.40–0.68). A significant overall group effect was found ($F_{(2,21)} = 5.894$; $P = 0.0093$) for the exploration ratio to differ between the groups. CYP animals subjected to exploration testing spent a significantly lower proportion of time exploring the original object compared with CON ($P = 0.013$) and CYP+hNSC ($P = 0.042$) groups (Fig. 1C). Furthermore, CON and CYP+hNSC groups did not differ statistically. Data indicate that hNSC transplantation improved exploration behavior after CYP treatment compared with CYP-treated animals not receiving stem cells.

Object in place

After TO testing, rats were habituated and tested in the OiP arena. Total exploration times of the objects followed similar trends as found in the TO task. Rats having intact cortical function will exhibit preference for those objects that have been switched to a novel location. While CON and CYP-hNSC cohorts showed preference for the objects placed at novel locations (Fig. 1D), neither was significantly different than CYP-treated animals. Furthermore, none of the cohorts explored novelty at levels significantly different than expected by chance (i.e., 50%).

For each of the foregoing open arena tasks, exploration ratios were normalized by the time spent at familiar locations and/or objects by calculating the discrimination index (DI), and in each case significant preference for the novelty was again found for the NPR and TO tasks with a trend in the OiP task (Supplementary

Table S1). While the overall tendency of CYP-treated cohorts was to explore less during the TO and OiP phases, the reduced exploration time was less likely to impact discrimination between the novel and familiar object (Supplementary Table S1). Since variations in overall exploration between the cohorts may, however, confound the assignment of exploration ratio data solely to cognitive deficits, additional analyses including locomotor activity and fear conditioning were conducted. While no changes were found in locomotor activity during habituation, CYP-treated cohorts did exhibit reduced locomotor activity compared with controls, an effect that was completely reversed by stem cell transplantation in all cohorts (Supplementary Data). Despite the beneficial effects of stem cell transplantation, these data prompted additional behavioral testing using a contextual FC task that does not rely on spontaneous exploration.

Fear conditioning

Each phase of the FC task (training, cue and context tests) were administered over 3 days. Group means and 95% CIs for post training and context phase freezing (percent) were as follows: post-training CON (mean = 98.6; 95% CI, 96–100); CYP (mean = 91.1; 95% CI, 87–95); CYP+hNSC (mean = 81.9; 95% CI, 69–94); context CON (mean = 64.6; 95% CI, 52–78); CYP (mean = 30.1; 95% CI, 22–38); CYP+hNSC (mean = 56.7; 95% CI, 44–69). Using repeated measures ANOVA, a significant overall group × phase interaction effect was found for the percentage of time spent freezing during the FC task (Fig. 1E; $F_{(8,84)} = 12.54$; $P = 0.0001$). Repeated measures two-way ANOVA for each phase revealed significant differences between CYP and Con groups in posttraining ($P = 0.022$) and context ($P = 0.002$) phases; and between CYP and CYP+hNSC groups in the context phase ($P = 0.04$). Groups did not differ significantly in the freezing behavior across baseline ($P = 0.25$), pre-cue ($P = 0.17$), and post-cue ($P = 0.12$) phases, indicating a selective deficit on the hippocampal-dependent contextual memory phase of the task. Transplanted animals were found to spend less time freezing during the post-training phase compared with controls ($P = 0.01$). During the context test phase, *post hoc* tests confirmed that CYP animals spent significantly decreased percentages of time freezing compared with CON ($P = 0.001$) and CYP+hNSC ($P = 0.002$) groups, whereas CON and CYP+hNSC groups did not differ. Moreover, because all groups showed significant increases in freezing behavior after the tone-shock pairings (posttraining phase), CYP treatment did not impair sensory function. As cued memory was intact, acquisition of the tone-shock pairing was not impaired, and the deficit was specific to the memory of the context in which the pairing was learned.

Survival and differentiation of grafted human cells

Confocal microscopy revealed the presence of surviving grafted human (HuN positive, green) cells in the hippocampus (Fig. 2A–C). The differentiated fate of graft-derived cells was determined by dual immunofluorescence and confocal Z-stack analyses (three representative sections/animal, $n = 4$ animals) of the CYP+hNSC cohort. Examination of dual immunofluorescence-stained HuN$^+$ cells revealed the majority of grafted cells to coexpress the neural stem cell marker (Fig. 2D, Sox2). Engrafted cells also differentiated along neuronal and astrocytic lineages. The analysis of dual-labeled cells indicated that multiple immature and mature
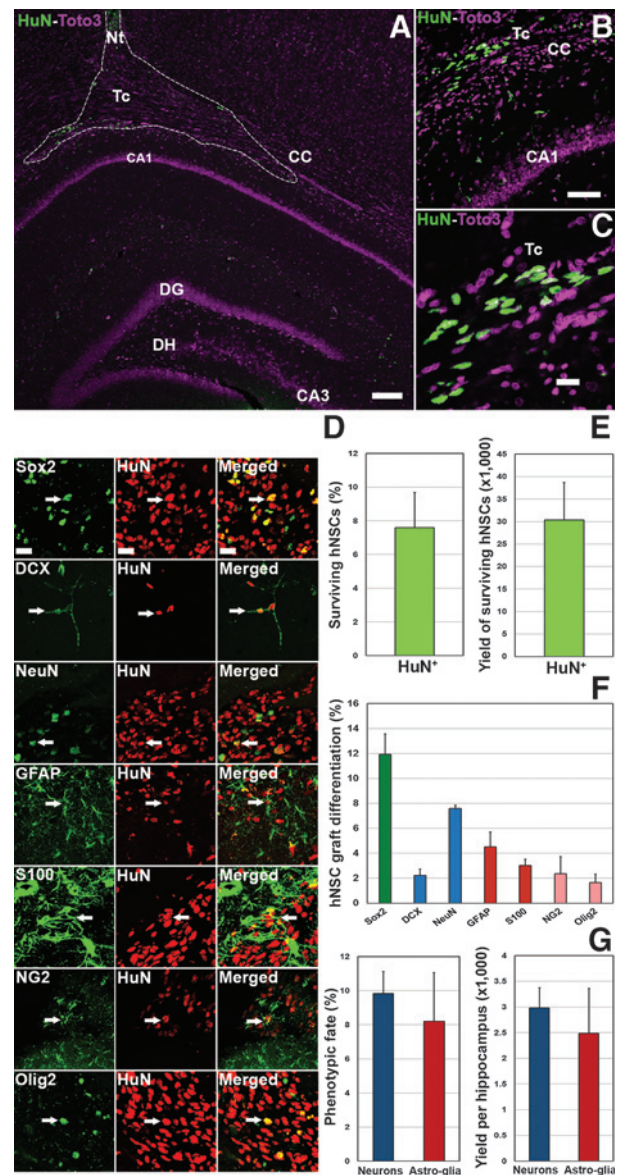

Figure 2.
Survival and differentiation of grafted hNSCs in CYP-treated brains. The majority of grafted human cells (HuN$^+$, green) was found ventral to the needle track (Nt) along the corpus callosum (CC) and dorsal to the CA1 subfield within the transplant core (Tc, dotted line; A), with smaller numbers of cells found migrating deeper within the CA1 (A). B and C, higher magnification confocal images showing the presence of grafted human cells within the CYP-treated brain (Toto3 nuclear counterstain, purple). D, differentiation of grafted human cells (HuN$^+$, red) as assessed by dual immunofluorescence staining of phenotypic markers (green). Data indicate the capability of grafted cells to commit to neuronal and astroglial lineages within the microenvironment of the chemotherapy treated brain. Despite relatively larger numbers of grafted cells retaining multipotency (Sox2), immature neurons (DCX), astrocytes (GFAP), and oligoprogenitors (NG2) were found along with their corresponding mature phenotypes (NeuN, S100, Olig2), respectively. Quantification of grafted cell survival by unbiased stereology (E), the yields of individual differentiated neural phenotypes (F), and the percentage and absolute numbers of graft-derived neurons and astroglia (G) are shown. All data are presented as means ± SEM ($N = 4$ animals per group); scale bar, 50 μm (A), 10 μm (B–C), and 5 μm (D).
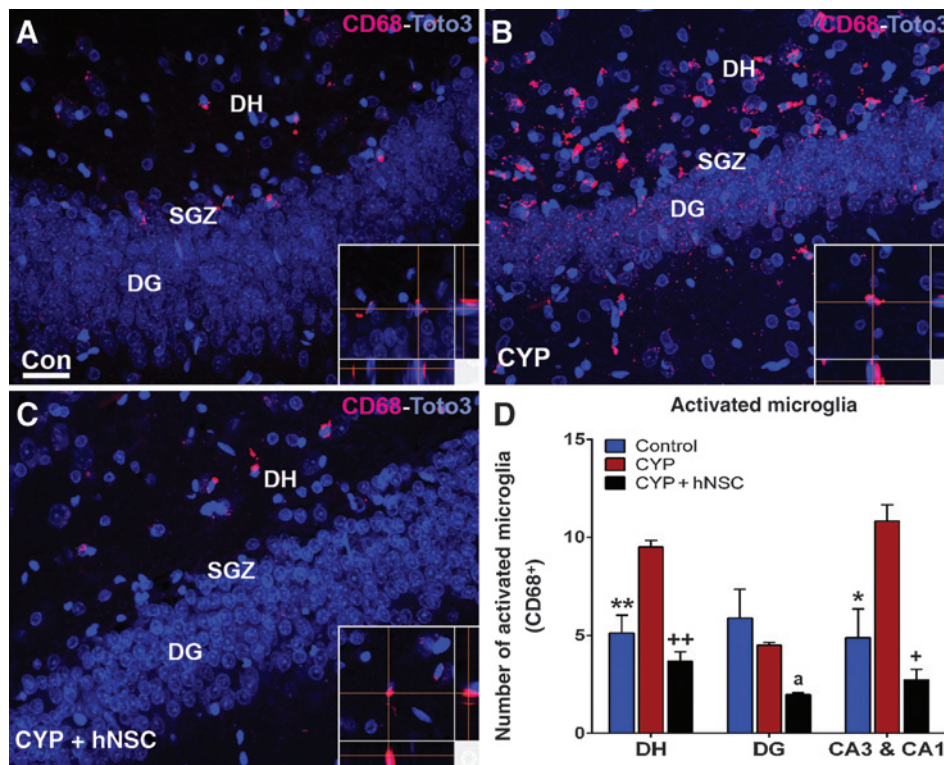
Figure 3.
Suppression of neuroinflammation following stem cell grafting. Immunohistochemical analysis shows that compared with controls (A), CYP treatment (B) leads to increased numbers of activated microglia (CD68$^+$, red; Toto3 nuclear counterstain, purple) that are reduced in animals receiving stem cells (C). Representative confocal images showing the presence of activated microglia in the hippocampal subfields of the DG, subgranular zone (SGZ), and DH, with orthogonal reconstructions (insets) of confocal Z-stacks (A–C). Quantification of activated microglia shows that compared with controls, CYP treatment significantly increased the number of activated microglia in the DH and CA3/CA1 subfields (D). Compared with CYP-treated cohorts, animals transplanted with stem cells (CYP+hNSC) were found to have significantly lower numbers of activated microglia in all hippocampal subfields analyzed. Reduced yields of activated microglia in the DH, DG, and CA3/CA1 regions were comparable (or lower) than untreated controls (D). All data are presented as means ± SEM ($N = 4$ animals per group). *, $P = 0.01$; **, $P = 0.001$; +, $P = 0.001$; ++, $P = 0.0001$ compared with CYP group; a, $P = 0.03$ compared with the control group (ANOVA and Bonferroni multiple comparison test). Scale bar, 50 μm (A–C) and 10 μm (insets).

neuronal, astrocytic and oligodendroglial phenotypes were present in the host hippocampus (Fig. 2D). Transplant-derived cells were found to express immature and mature neuron (DCX and NeuN), astrocyte (GFAP and S100β$^+$) and oligodendrocytes (NG2 and Olig2) markers (Fig. 2D). Unbiased stereology used to quantify the number of surviving grafted human cells revealed that 7.59% ± 2.09% (mean ± SEM, $n = 4$ animals) or 30,340 ± 8,370 (mean ± SEM, $n = 4$ animals) cells remained 2 months following transplantation surgery (Fig. 2E).

Quantification of differentiated phenotypes revealed that the majority of graft-derived cells (percentage of HuN$^+$ cells) expressed Sox2 (11.9% ± 1.6%, $N = 4$). Immature (DCX, 2.22% ± 0.51%; $N = 4$) and mature (NeuN, 7.61% ± 0.25%; $N = 4$) neurons, immature (GFAP, 4.52% ± 1.2%; $N = 4$) and mature (S100, 3.02% ± 0.50%; $N = 4$) astrocytes, and oligoprogenitors (NG2, 2.37% ± 1.4%; $N = 4$) and mature (Olig2, 1.65% ± 0.69%; $N = 4$) oligodendrocytes were also found (Fig. 2F). Collectively, these yields translated to 9.83 ± 1.3% or 2,980 ± 388 neurons and 8.20 ± 2.9% or 2,490 ± 871 astroglia per hippocampus surviving 2 months after transplantation (Fig. 2G). Thus, chemotherapy exposure did not impose any overt restrictions on lineage-specific progression, as stem cells were able to graft and differentiate within a permissive microenvironment.

Neuroinflammation

We reported previously that exposure to chemotherapy elevates neuroinflammation (4), and to assess the impact of CYP and stem cell treatments on the inflammatory status of the brain, microglia were quantified throughout different regions of the hippocampus (Fig. 3A–C). A significant overall group effect was found for differences in the number of activated microglia in the dentate hilus (DH; $F_{(2,9)} = 32.67$, $P = 0.0001$), the dentate gyrus (DG; $F_{(2,7)} = 6.343$, $P = 0.0268$) and the CA1/3 subfields ($F_{(2,8)} = 22.46$, $P = 0.0005$). Compared with controls, CYP treatment elevated the number of activated microglia (ED1$^+$ cells) significantly in the DH and CA3/1 subfields, an effect not found in the DG (Fig. 3D). Stem cell grafting was found to reduce significantly the number of activated microglia in the DH, DG, and the CA3/1 subfields (Fig. 3D). Data indicate that stem cell grafting significantly reduced neuroinflammation in each of the hippocampal subfields analyzed.

Neuronal morphology in the dentate gyrus

Past work has shown that chemotherapy disrupted the architecture of newly born neurons (4). To elucidate more completely the effects of CYP treatment on the structure of more mature

Figure 4.
Transplantation of hNSCs protects granule cell neuronal morphology in the DG. Representative images of Golgi–Cox impregnated hippocampal tissue sections from control (A), CYP (B), and CYP+hNSC (C) cohorts reveals the gross disruption to neuronal structure (black) in the DG and CA1 subfields of the hippocampus (nuclear fast red counterstained) caused by CYP treatment that is resolved in animals receiving stem cells. D, representative tracings of granule cell neurons from each cohort superimposed over concentric Sholl circles (20 μm increments). E, structural parameters of dendritic morphology (length, volume, complexity) quantified in each cohort showing the CYP-induced reductions in dendritic morphology that were ameliorated by stem cell grafting. Data are presented as means ± SEM ($N = 4$ animals per group). $*$, $P = 0.001$; $**$, $P = 0.0001$; $+$, $P = 0.01$; $++$, $P = 0.0004$ compared with CYP group (ANOVA and Bonferroni multiple comparison test). Scale bar, 200 μm (A–C).
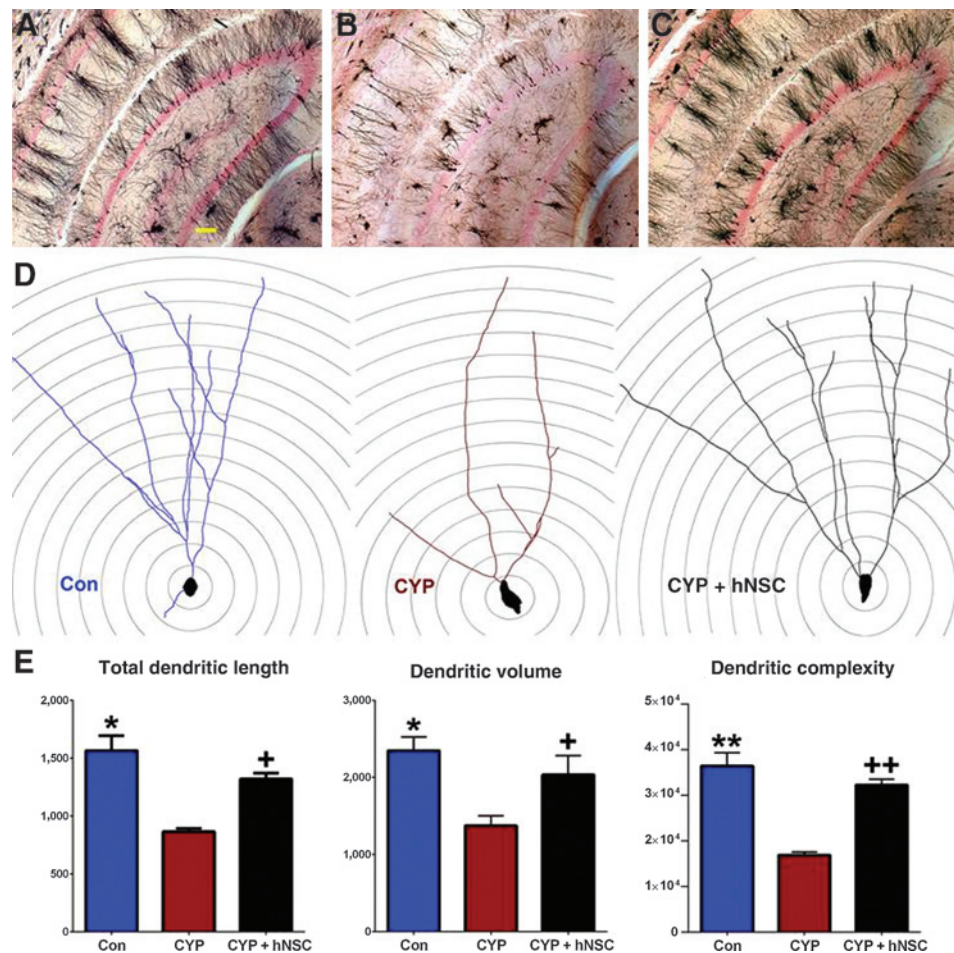
neurons in the DG, Golgi–Cox impregnated sections were analyzed for changes in dendritic structure, spine density and morphology. Wide field images of Golgi–Cox impregnated neurons in the DG and CA1 hippocampal subfields reveal the marked impact of CYP treatment (Fig. 4A–C). Compared with controls (Fig. 4A), neuronal complexity is severely compromised after exposure to CYP (Fig. 4B) an adverse effect that is reversed by stem cell grafting (Fig. 4C). Representative neuronal tracings from each cohort are shown superimposed over concentric Sholl circles spaced 50 μm apart (Fig. 4D). Dendritic tracing of granule cell neurons revealed the adverse effects of chemotherapy and the beneficial effects of stem cell grafting on neuronal morphology. Significant overall group effects were found for dendritic length ($F_{(2,9)} = 19.07$; $P = 0.0006$), volume ($F_{(2,9)} = 11.74$; $P = 0.0031$), and complexity ($F_{(2,0)} = 35.44$; $P = 0.0001$). Quantification of dendritic parameters revealed that CYP cohorts exhibited significant reductions in overall dendritic length, volume and complexity compared with the other cohorts (Fig. 4E). Significant overall group effects were also found for changes in dendritic endings ($F_{(2,9)} = 17.82$; $P = 0.0007$), granule neuron cell body area ($F_{(2,9)} = 6.491$; $P = 0.018$) and soma perimeter ($F_{(2,9)} = 40.18$; $P = 0.0001$). Compared with the other cohorts, CYP-treated animals exhibited reduced dendritic endings and a marked swelling of the cell body (Supplementary Fig. S2A). Furthermore, Sholl analyses showed that CYP treatments reduced significantly the number of distal

dendritic endings and intersections (100–200 μm) from the soma with smaller effects on the number of dendritic nodes (Supplementary Fig. S2B). For all the foregoing endpoints, sham-surgery controls (CON) were statistically indistinguishable from those animals receiving stem cell transplants (CYP+hNSC). Data show that stem cell grafting preserved host dendritic structure following chemotherapy.

Neuronal morphology in the CA1

Similar morphometric analyses were conducted in the CA1 subfield to assess the impact of CYP and stem cell treatments on pyramidal neurons. As before, overall dendritic arborization was reduced significantly in CYP-treated animals compared with other cohorts, evident in the representative tracings of pyramidal cell neurons (Fig. 5A). Further analysis of the basal dendritic tree revealed significant overall group effects for changes in the total dendritic length ($F_{(2,9)} = 24.73$; $P = 0.0002$), volume ($F_{(2,9)} = 50.89$; $P = 0.0001$), and complexity ($F_{(2,9)} = 21.73$; $P = 0.0004$; Fig. 5B). These data showed that CYP led to significant reductions in overall dendritic length, volume, and complexity compared with the other cohorts (Fig. 5B). As in the DG, significant overall group effects were found for changes in basal dendritic endings ($F_{(2,9)} = 9.382$; $P = 0.0063$) and in pyramidal neuron soma perimeter ($F_{(2,9)} = 35.40$; $P = 0.0001$), where CYP-treated animals were found to have lower dendritic endings and
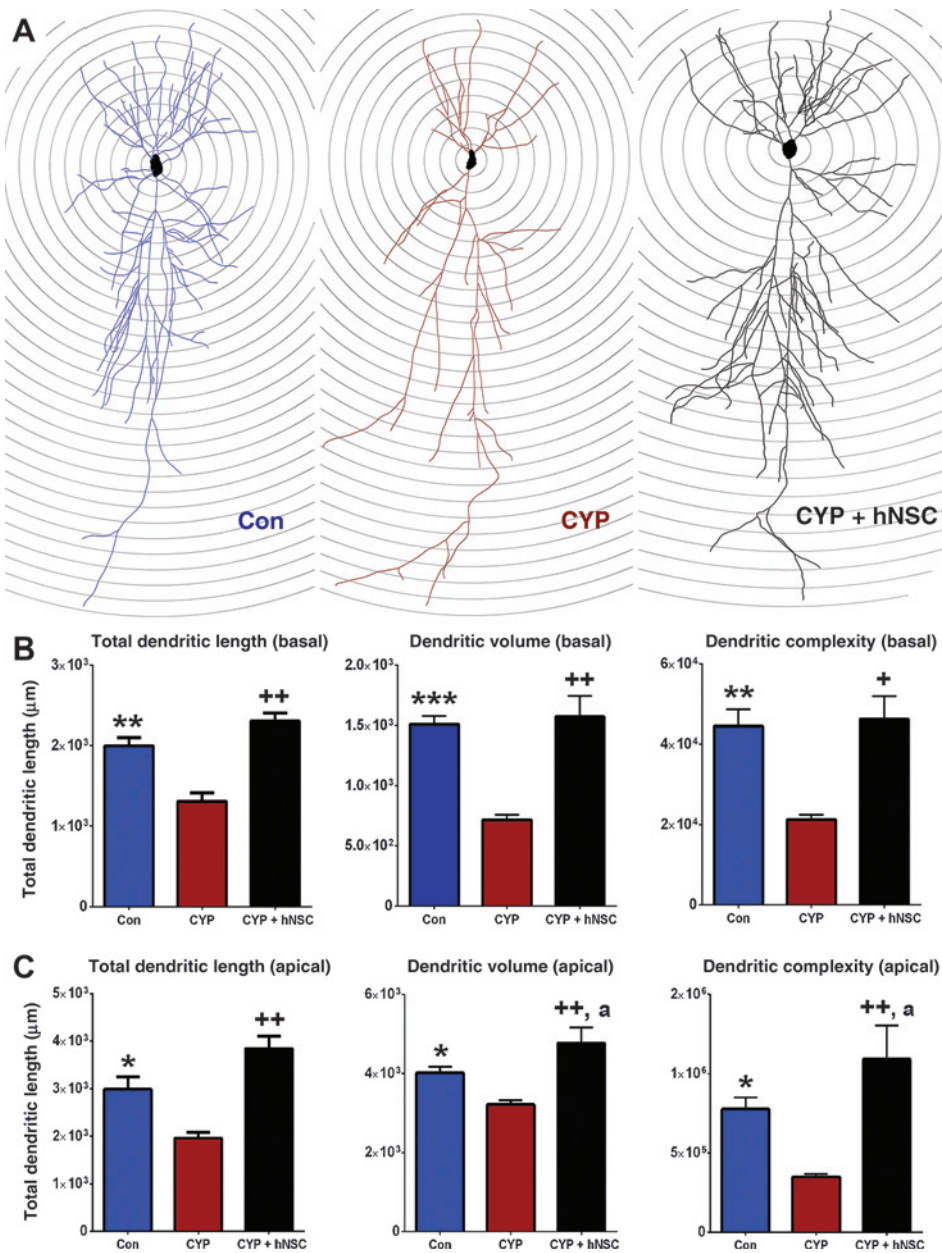
Figure 5.
Transplantation of hNSCs protects pyramidal neuronal architecture in the CA1. A, representative tracings of the basal and apical dendritic tress of CA1 pyramidal cell neurons from each cohort superimposed over concentric Sholl circles (20 μm increments). B and C, structural parameters of basal and apical dendritic morphology (length, volume, complexity) quantified in each cohort showing CYP-induced reductions in dendritic morphology that were ameliorated by stem cell grafting. Data are presented as means $\pm$ SEM ($N = 4$ animals each group). *, $P = 0.01$; **, $P = 0.001$; ***, $P = 0.0001$; +, $P = 0.001$; ++, $P = 0.0002$, compared with CYP group; a, $P = 0.05$ compared with the control group (ANOVA and Bonferroni multiple comparison test).

swollen soma (Supplementary Fig. S3A and S3B). Sholl analyses showed that CYP reduced significantly the number of proximal dendritic endings and intersections (50–200 μm) from the soma with little impact on the number of dendritic nodes (Supplementary Fig. S3C) in the basal tree. For basal dendritic parameters, sham-surgery controls (CON) were statistically indistinguishable from those animals receiving stem cell transplants (CYP+hNSC).

Analogous measurements conducted on the apical dendritic tree revealed qualitatively similar effects. Significant overall groups effects were again found for changes in dendritic length ($F_{(2,9)} = 18.5$; $P = 0.0006$), volume ($F_{(2,9)} = 22.89$; $P = 0.0003$), and complexity ($F_{(2,9)} = 24.51$; $P = 0.0002$; Fig. 5B), in addition to dendritic endings ($F_{(2,9)} = 13.74$; $P = 0.0018$; Supplementary Fig. S3A). Analysis of apical dendritic morphology showed that CYP

treatments caused significant reductions in total dendritic length, volume, complexity (Fig. 5B), and endings (Supplementary Fig. S3) compared with control and transplanted (CYP+hNSC) cohorts. Stem cell grafting was again found to significantly increase each of these dendritic parameters compared with the other cohorts (Fig. 5B and Supplementary Fig. S3). Sholl analyses also revealed that CYP treatment led to marked and significant reductions in the number of dendritic endings, intersections, and nodes over proximal distances (100–300 μm) from the soma (Supplementary Fig. S3D). Collectively, morphometric data indicate clearly that following chemotherapy stem cell transplantation had a significant and beneficial effect that involved the enhanced arborization of the apical and basal dendritic trees of CA1 pyramidal cells.
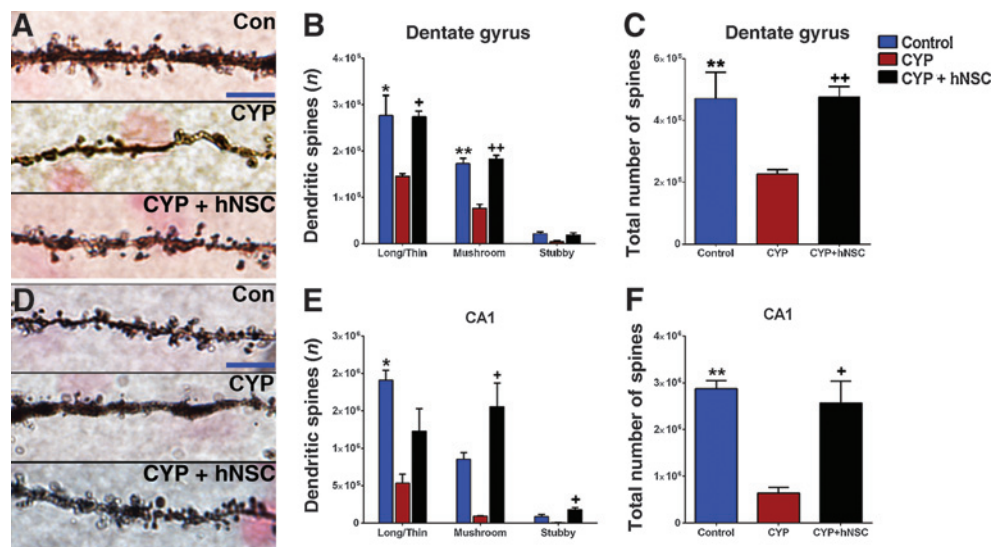
Figure 6.
Stem cell grafting preserves dendritic spine density and the number of immature and mature spine morphologies following chronic chemotherapy. Representative images from each cohort showing dendritic spines along Golgi–Cox impregnated granule cell (A) or pyramidal (D) neurons in the DG or CA1 subfields respectively. Quantification of spine morphologies by unbiased stereology shows significantly reduced numbers of both immature (long/thin, mushroom) and mature (stubby) spines in the DG (B) or CA1 (E) of CYP-treated animals compared with control and grafted cohorts. The total spine density is reduced significantly in the DG (C) and CA1 (F) of CYP-treated animals compared with either control or CYP+hNSC cohorts. All data are presented as means ± SEM ($N = 3$ animals each group). *, $P = 0.01$; **, $P = 0.001$; +, $P = 0.01$; ++, $P = 0.001$ compared with CYP group (ANOVA and Bonferroni multiple comparison test). Scale bar, 5 μm (A and D).

Dendritic spine analysis in the dentate gyrus and CA1

Analysis of dendritic spines along neurons within the DG and CA1 subfields again showed the significant adverse effects of CYP treatment when compared against untreated or stem cell–grafted cohorts (Fig. 6). Representative images of selected dendritic segments in the DG and CA1 (Fig. 6A and D) show the stripping of synaptic spines caused by CYP treatments, which was reversed by stem cell grafting. Stereologic quantification of immature and mature spine morphologies along granule and pyramidal cell neurons (Fig. 6B and E) show that compared with the other cohorts, chemotherapy caused marked and significant reductions in all spine types. Significant overall group effects were found for changes in the number of long/thin ($F_{(2,6)} = 8.301$; $P = 0.0187$) and mushroom ($F_{(2,6)} = 40.25$; $P = 0003$) spine types in the DG, with a trend ($F_{(2,6)} = 4.969$, $P = 0.0534$) found for stubby spines (Fig. 6B). Similarly, overall group effects were found for altered numbers of long/thin ($F_{(2,6)} = 12.04$; $P = 0.0079$), mushroom ($F_{(2,6)} = 14.84$; $P = 0.0048$), and stubby ($F_{(2,6)} = 13.52$; $P = 0.006$) spine types in the CA1 (Fig. 6E). Importantly, reductions in the number of specific spine types after CYP treatment translated to significant overall group effects for the number of total spines in the DG ($F_{(2,6)} = 21.91$; $P = 0.0017$) and CA1 ($F_{(2,6)} = 16.70$; $P = 0.0035$) subfields (Fig. 6C and F). Dendritic spine density in the DG and CA1 was reduced significantly in CYP-treated animals compared with control and transplanted (CYP+hNSC) cohorts (Fig. 6C and F). These data demonstrate that in addition to the preservation of dendritic architecture, stem cell grafting increased immature and mature spine numbers to enhance spine density after chemotherapy.

Discussion

Adverse neurocognitive side effects associated with various chemotherapy regimens have now been recognized clinically for many years (25). Diverse and multifaceted decrements involving memory, concentration, language, attention, and executive function have been described that impact multiple cognitive domains that persist long after the cessation of chemotherapy (26). While animal work conducted in the absence of confounding disease has shed considerable light on many factors contributing to chemobrain, the mechanisms underlying this serious clinical disorder remain incompletely understood. Thus, the current work sought to identify potential neurobiologic mechanisms involved in chemobrain as well as to explore the use of stem cells as potential therapeutic agents to reverse and/or protect against the neurocognitive sequelae associated with this condition.

Cognitive tasks were selected to specifically interrogate medial prefrontal cortical function as well as hippocampal dependent tasks. Chronic CYP treatment was shown to significantly impair behavioral performance on 3 of 4 cognitive tasks administered (Fig. 1). Arena testing revealed significant impairments on the NPR and TO tasks with a similar trend found on the OIP task. Permanent lesion studies have established the importance of the perirhinal cortex, medial prefrontal cortex and hippocampus in TO and OIP recognition memory (27, 28). Performance on these tasks also requires circuits from these three regions to interact (27, 28), suggesting that chronic CYP treatment disrupted neural connectivity between hippocampal and cortical circuits. Exploration ratios (Fig. 1) and Supplementary Data shown as DIs show a clear preference for the novel object (NPR and TO tasks), and the similarity of time spent exploring either object on the NPR task

suggest these deficits are likely the result of impaired hippocampal learning and memory. For the TO and OiP tasks, the total time exploring novel and familiar objects were found to exhibit some variation, as the total exploration for the control group was relatively high (and statistically different) compared with either CYP or CYP+hNSC groups. While this may indicate that CYP-treated animals simply did not recognize that the arrangement of objects/locations was different and so, did not possess the same level of curiosity to explore a "new" environment, other factors such as depression and/or anxiety may be associated with the behavioral decrements on these tasks. Nonetheless, such effects were still ameliorated by stem cell transplantation in all cohorts.

While the focus of this study was not to elucidate the sensitivity of different brain regions to CYP, as treatments were systemic, these data do corroborate certain clinical findings (29, 30), and demonstrate that CYP treatments likely induced more global insults to the brain not merely restricted to the hippocampus. FC was conducted in part to ensure that reduced locomotor activity was not differentially affecting exploration preference between the cohorts. Data confirmed that CYP treatment caused a significant impairment on the hippocampal-dependent contextual memory test, an effect that did not extend to cued memory that has been shown to be more dependent on the amygdala (31).

Unbiased stereology used to quantify grafted cell survival confirmed that 8% of the transplanted cells were still present 2 months after surgery (Fig. 2). These data indicate that exposure to chronic CYP did not preclude stem cell grafting or render the CNS microenvironment refractory to the beneficial effects of stem cell transplantation. Cells surviving at this time were found to express both immature and mature markers of neuronal and astroglial lineages along with markers of multipotency (Fig. 2). It is noteworthy that so few cells (i.e., ~60,000/brain) were able to provide such extensive neurocognitive benefits, suggesting that transplanting fewer rather than greater numbers of stem cells may provide equivalent (or superior) beneficial effects. On the basis of phenotype, morphology, location, distance from transplant core and yield, the beneficial CNS effects associated with stem cell grafting appear more likely the result of trophic support, rather than functional replacement. Finally, the impact of grafted cells on host neurogenesis may also play a role in mediating certain positive effects of stem cell grafting in the CYP-treated brain, and while not a focus of this study, we cannot formally discount this possibility.

To analyze further the potential mechanisms by which grafted cells nurture and/or protect the host microenvironment, the number of microglia were quantified to gauge relative levels of neuroinflammation between cohorts and different regions of the brain. With the exception of the DG, CYP treatment caused a significant (~2-fold) rise in activated microglia compared with controls (Fig. 3). For all cohorts, stem cell grafting reduced significantly, the number of activated microglia compared with CYP-treated cohorts, and showed a trend toward reduced microglia compared to controls. Thus, the capability of grafted stem cells to attenuate neuroinflammation provides one plausible explanation for their beneficial effects in the CYP-treated brain, and likely involves the quenching of chemokine signaling in the brain to dampen the recruitment and/or activation of resident microglia (32, 33).

Suppression of neuroinflammation can have a variety of pleiotropic effects (34), where microglia have been found to regulate synaptic plasticity by actively pruning neuronal circuits to main-

tain dendritic structure and synaptic function (35–37). In response to chemotherapy, endogenous microglia may be activated to remodel damage circuits and synaptic connections, resulting in reduced dendritic complexity and spine density. To test this, neuronal architectural parameters were quantified within the DG and CA1 subfields and data revealed significant reductions in dendritic arborization and spine density (Figs. 4–6 and Supplementary Figs. S1 and S2). Overall, dendritic length, volume and complexity were reduced significantly by CYP treatments, effects that were preserved at control levels in cohorts receiving stem cell transplantation. Sholl analyses corroborated these results, showing that granule and pyramidal cell neurons from each region of CON and CYP-hNSC cohorts exhibited a significant increase in the number of dendritic endings and/or intersections over proximal to distal distances from the soma compared with CYP-treated cohorts. Collectively, data demonstrate that stem cell grafting either protected host neuronal circuitry or promoted recovery following CYP treatment.

The beneficial effect of stem cells extended to the ultrastructural features of dendrites as reductions in spine density and critical morphologies caused by CYP, were also resolved by stem cell grafting. In the DG, exposure to CYP led to significant reductions in spine density and specific spine morphologies. In the CA1, chronic CYP treatments caused significant reductions in mushroom and stubby spine morphologies with a trend toward reduced long/thin spines. These changes again translated to an overall significant reduction in spine density (Fig. 6). Interestingly, CYP treatment induced a significant swelling of the cell body in neurons of the DG and CA1 compared with the other cohorts. Past work (38) has documented hypertrophy of the soma associated with other neuropathologic conditions, and current findings suggest that chemotherapy elicits a similar response. In each of the foregoing instances, stem cell grafting promoted the recovery of overall spine density and each of the CYP-depleted spine morphologies. Thus, in addition to the improvements in dendritic arborization, stem cell grafting had a significant and beneficial impact on dendritic spines, where both immature (long/thin, mushroom) as well as mature (stubby) morphologies depleted by CYP treatments returned to levels at or higher than control levels following stem cell grafting.

A wealth of past studies has established a clear link between a variety of neurodegenerative conditions, including aging, and disrupted neuronal morphology (20, 39, 40). Alterations to dendritic arborization, synaptic integrity, spine density, and morphology have been found in all neurodegenerative diseases associated with deficits in learning and memory (41–43). As evidence indicates that compromised dendritic structure and synaptic plasticity hastens the onset and severity of neurocognitive sequelae, it is not surprising that chemotherapy-associated cognitive decline exhibits similar structural and functional parallels with other conditions of cognitive dysfunction, especially when compared with other treatments (e.g., radiotherapy) used to control the growth and spread of cancer (16, 17).

Our preclinical data shed considerable light on the causes and potential treatments for chemobrain in two important ways. First, chemotherapy-induced hippocampal and cortical behavioral deficits are directly associated with compromised neuronal architecture, depleted dendritic spines, and elevated yields of activated microglia in the hippocampus. Second, the neuropathology associated with chemobrain can be reversed successfully via cranial transplantation of hNSCs, leading to functional improvements in

behavior. Whether this effect was the consequence of suppressing neuroinflammation and/or stimulating dendritic branching and spinogenesis through secreted neurotrophic factors remains uncertain, but our data demonstrate clearly that a wide range of adverse effects associated with a chronic chemotherapy regimen can be improved significantly at the cellular, structural, and functional levels by stem cell transplantation.

Disclosure of Potential Conflicts of Interest

No potential conflicts of interest were disclosed.

Authors' Contributions

Conception and design: M.M. Acharya, V. Martirosian, L.-A. Christie, V.K. Parihar, C.L. Limoli
Development of methodology: M.M. Acharya, V. Martirosian, N. Hanna, L.-A. Christie, V.K. Parihar, C.L. Limoli
Acquisition of data (provided animals, acquired and managed patients, provided facilities, etc.): M.M. Acharya, V. Martirosian, N. Hanna, K.K. Tran, A.C. Liao, V.K. Parihar
Analysis and interpretation of data (e.g., statistical analysis, biostatistics, computational analysis): M.M. Acharya, V. Martirosian, N.N. Chmielewski, N. Hanna, V.K. Parihar, C.L. Limoli
Writing, review, and/or revision of the manuscript: M.M. Acharya, V. Martirosian, N. Hanna, L.-A. Christie, V.K. Parihar, C.L. Limoli
Administrative, technical, or material support (i.e., reporting or organizing data, constructing databases): V. Martirosian, N.N. Chmielewski, N. Hanna
Study supervision: V. Martirosian, N. Hanna, C.L. Limoli

Grant Support

References

1. Valdivieso M, Kujawa AM, Jones T, Baker LH. Cancer survivors in the United States: a review of the literature and a call to action. Int J Med Sci 2012; 9:163–73.
2. Ahles TA, Saykin AJ, Furstenberg CT, Cole B, Mott LA, Skalla K, et al. Neuropsychologic impact of standard-dose systemic chemotherapy in long-term survivors of breast cancer and lymphoma. J Clin Oncol 2002; 20:485–93.
3. Wefel JS, Saleeba AK, Buzdar AU, Meyers CA. Acute and late onset cognitive dysfunction associated with chemotherapy in women with breast cancer. Cancer 2010;116:3348–56.
4. Christie LA, Acharya MM, Parihar VK, Nguyen A, Martirosian V, Limoli CL. Impaired cognitive function and hippocampal neurogenesis following cancer chemotherapy. Clin Can Res 2012;18:1954–65.
5. Fardell JE, Vardy J, Johnston IN. The short and long term effects of docetaxel chemotherapy on rodent object recognition and spatial reference memory. Life Sci 2013;93:596–604.
6. Nokia MS, Anderson ML, Shors TJ. Chemotherapy disrupts learning, neurogenesis and theta activity in the adult brain. Eur J Neurosci 2012; 36:3521–30.
7. Palmer SL, Reddick WE, Gajjar A. Understanding the cognitive impact on children who are treated for medulloblastoma. J Pediat Psychol 2007; 32:1040–9.
8. Saury JM, Emanuelson I. Cognitive consequences of the treatment of medulloblastoma among children. Pediat Neurol 2011;44:21–30.
9. Krull KR, Brinkman TM, Li C, Armstrong GT, Ness KK, Srivastava DK, et al. Neurocognitive outcomes decades after treatment for childhood acute lymphoblastic leukemia: a report from the St Jude lifetime cohort study. J Clin Oncol 2013;31:4407–15.
10. Boykoff N, Moieni M, Subramanian SK. Confronting chemobrain: an in-depth look at survivors' reports of impact on work, social networks, and health care response. J Cancer Surviv 2009;3:223–32.
11. Joly F, Rigal O, Noal S, Giffard B. Cognitive dysfunction and cancer: which consequences in terms of disease management? Psychooncology 2011 20:1251–8.
12. Myers JS. Chemotherapy-related cognitive impairment. Clin J Oncol Nurs 2009;13:413–21.
13. Ahles TA, Saykin AJ. Candidate mechanisms for chemotherapy-induced cognitive changes. Nat Rev Cancer 2007;7:192–201.
14. Mizumatsu S, Monje M, Morhardt D, Rola R, Palmer T, Fike J. Extreme sensitivity of adult neurogenesis to low doses of X-irradiation. Cancer Res 2003;63:4021–7.
15. Seigers R, Schagen SB, Coppens CM, van der Most PJ, van Dam FS, Koolhaas JM, et al. Methotrexate decreases hippocampal cell proliferation and induces memory deficits in rats. Behav Brain Res 2009;201:279–84.
16. Parihar VK, Limoli CL. Cranial irradiation compromises neuronal architecture in the hippocampus. Proc Natl Acad Sci U S A 2013; 110:12822–7.
17. Parihar VK, Pasha J, Tran KK, Craver BM, Acharya MM, Limoli CL. Persistent changes in neuronal structure and synaptic plasticity caused by proton irradiation. Brain Struct Func 2014 Jan 21. [Epub ahead of print].
18. Tseng BP, Giedzinski E, Izadi A, Suarez T, Lan ML, Tran KK, et al. Functional consequences of radiation-induced oxidative stress in cultured neural stem cells and the brain exposed to charged particle irradiation. Antioxid Redox Signal 2013;20:1410–22.
19. Bremner JD, Krystal JH, Southwick SM, Charney DS. Functional neuroanatomical correlates of the effects of stress on memory. J Traumat Stress 1995;8:527–53.
20. Kaufmann WE, Moser HW. Dendritic anomalies in disorders associated with mental retardation. Cereb Cortex 2000;10:981–91.
21. Terry RD, Peck A, DeTeresa R, Schechter R, Horoupian DS. Some morphometric aspects of the brain in senile dementia of the Alzheimer type. Ann Neurol 1981;10:184–92.
22. Acharya MM, Christie LA, Lan ML, Giedzinski E, Fike JR, Rosi S, et al. Human neural stem cell transplantation ameliorates radiation-induced cognitive dysfunction. Cancer Res 2011;71:4834–45.
23. Acharya MM, Lan ML, Kan VH, Patel NH, Giedzinski E, Tseng BP, et al. Consequences of ionizing radiation-induced damage in human neural stem cells. Free Radic Biol Med 2010;49:1846–55.
24. Acharya MM, Christie LA, Lan ML, Donovan PJ, Cotman CW, Fike JR, et al. Rescue of radiation-induced cognitive impairment through cranial transplantation of human embryonic stem cells. Proc Natl Acad Sci U S A 2009;106:19150–5.
25. Wefel JS, Schagen SB. Chemotherapy-related cognitive dysfunction. Curr Neurol Neurosci Rep 2012;12:267–75.
26. Dietrich J, Monje M, Wefel J, Meyers C. Clinical patterns and biological correlates of cognitive dysfunction associated with cancer therapy. Oncologist 2008;13:1285–95.
27. Barker GR, Bird F, Alexander V, Warburton EC. Recognition memory for objects, place, and temporal order: a disconnection analysis of the role of the medial prefrontal cortex and perirhinal cortex. J Neurosci 2007;27: 2948–57.
28. Barker GR, Warburton EC. When is the hippocampus involved in recognition memory? J Neurosci 2011;31:10721–31.
29. Evenden J. Cognitive impairments and cancer chemotherapy: translational research at a crossroads. Life Sci 2013;93:589–95.
30. Seigers R, Fardell JE. Neurobiological basis of chemotherapy-induced cognitive impairment: a review of rodent research. Neurosci Biobehav Rev 2011;35:729–41.

31. Phillips RG, LeDoux JE. Differential contribution of amygdala and hippocampus to cued and contextual fear conditioning. Behav Neurosci 1992;106:274–85.

32. Belarbi K, Arellano C, Ferguson R, Jopson T, Rosi S. Chronic neuroinflammation impacts the recruitment of adult-born neurons into behaviorally relevant hippocampal networks. Brain Behav Immun 2012;26:18–23.

33. Talaveron R, Matarredona ER, de la Cruz RR, Macias D, Galvez V, Pastor AM. Implanted neural progenitor cells regulate glial reaction to brain injury and establish gap junctions with host glial cells. Glia 2014;62:623–38.

34. Ekdahl CT. Microglial activation - tuning and pruning adult neurogenesis. Front Pharmacol 2012;3:41.

35. Paolicelli RC, Bolasco G, Pagani F, Maggi L, Scianni M, Panzanelli P, et al. Synaptic pruning by microglia is necessary for normal brain development. Science 2011;333:1456–8.

36. Wake H, Moorhouse AJ, Miyamoto A, Nabekura J. Microglia: actively surveying and shaping neuronal circuit structure and function. Trends Neurosci 2013;36:209–17.

37. Ji K, Akgul G, Wollmuth LP, Tsirka SE. Microglia actively regulate the number of functional synapses. PLoS ONE 2013;8:e56293.

38. Colciaghi F, Finardi A, Nobili P, Locatelli D, Spigolon G, Battaglia GS. Progressive brain damage, synaptic reorganization and NMDA activation in a model of epileptogenic cortical dysplasia. PLoS ONE 2014;9: e89898.

39. Peters A, Kemper T. A review of the structural alterations in the cerebral hemispheres of the aging rhesus monkey. Neurobiol Aging 2012;33: 2357–72.

40. van Spronsen M, Hoogenraad CC. Synapse pathology in psychiatric and neurologic disease. Curr Neurol Neurosci Rep 2010;10:207–14.

41. Pfeiffer BE, Huber KM. The state of synapses in fragile X syndrome. Neuroscientist 2009;15:549–67.

42. Selkoe DJ. Alzheimer's disease is a synaptic failure. Science 2002;298: 789–91.

43. Yuste R, Bonhoeffer T. Genesis of dendritic spines: insights from ultrastructural and imaging studies. Nat Rev Neurosci 2004;5:24–34.

AACR American Association for Cancer Research

Stem Cell Transplantation Reverses Chemotherapy-Induced Cognitive Dysfunction

Munjal M. Acharya, Vahan Martirosian, Nicole N. Chmielewski, et al.

Cancer Res 2015;75:676-686.

Updated version	Access the most recent version of this article at: http://cancerres.aacrjournals.org/content/75/4/676

Cited Articles	This article cites by 42 articles, 14 of which you can access for free at: http://cancerres.aacrjournals.org/content/75/4/676.full.html#ref-list-1

E-mail alerts	Sign up to receive free email-alerts related to this article or journal.
Reprints and Subscriptions	To order reprints of this article or to subscribe to the journal, contact the AACR Publications Department at pubs@aacr.org.
Permissions	To request permission to re-use all or part of this article, contact the AACR Publications Department at permissions@aacr.org.